Journal of Southeast University (English Edition) Vol. 27, No. 4, pp. 394 – 399 Dec. 2011 ISSN 1003—7985

Local hierarchical non-negative tensor factorization and its application in machinery fault diagnosis

Wang Fei[1] Xu Feiyun[2] Wang Haijun[2]

(School of Mechanical Engineering, Southeast University, Nanjing 211189, China)

Abstract: Aiming at the slow convergence and low accuracy problems of the traditional non-negative tensor factorization, a local hierarchical non-negative tensor factorization method is proposed by applying the local objective function theory to non-negative tensor factorization and combining the three semi-non-negative matrix factorization (NMF) model. The effectiveness of the method is verified by the facial feature extraction experiment. Through the decomposition of a series of an air compressor's vibration signals composed in the form of a bispectrum by this new method, the basis images representing the fault features and corresponding weight matrices are obtained. Then the relationships between characteristics and faults are analyzed and the fault types are classified by importing the weight matrices into the BP neural network. Experimental results show that the accuracy of fault diagnosis is improved by this new method compared with other feature extraction methods.

Key words: non-negative tensor factorization; bispectrum; feature extraction; air compressor; BP neural network

doi: 10.3969/j.issn.1003 – 7985.2011.04.010

Many traditional methods are widely used in feature extraction, such as principal component analysis (PCA), singular value decomposition (SVD), independent component analysis (ICA), and so on. They are mainly used to deal with two-dimensional data but powerless to deal with multi-dimensional data. For the purpose of multi-dimensional data feature extraction, the common method is to transform the data into a two-dimensional form and then extract the features. The extracted features are re-transformed into the previous dimension. Through the method above, the original data structure is destroyed to some extent and cannot reflect the relevance of time and space. Furthermore, the decomposition often done in one step is not accurate. As a result, the feature cannot well reflect the information contained in the data.

Non-negative tensor factorization (NTF) is the sum of a series of tensors (rank 1) formed by the out-product of several vectors, which can achieve a high decomposition accuracy and give unique results even in weak cases, owing to the fact that it considers the relationships of variables in space and time. The result is unique, more sparse, and has a more accurate representation of the local features compared with those by the traditional methods.

In recent years, much attention has been paid to the research of NTF. Hazan et al.[1] proposed an iterative algorithm of the NTF based on the gradient descent method. Cichocki et al.[2] applied the divergence based HALS to the NTF and gave a detailed formula. Through dealing with the swimmer data and human brain waves, a high fit degree of the algorithm was verified by comparing it with other methods. According to the nature of sparseness-constrained non-negative matrix factorization (NMF), Heiler and Schnörr[3] proposed a sparse NTF algorithm based on the second-order cone, which can extract more sparse features compared with the method based on the Euclidean distance. Park et al.[4] introduced a multi-linear tensor decomposition and applied it to face recognition. However, there has not been a great breakthrough with respect to the problems of slow convergence, multiple iterations and low precision of the NTF. Furthermore, there is also not much coverage about the NTF applied to mechanical fault extraction and diagnosis.

In this paper, after summarizing the previous theories and the existing problems of the NTF, hierarchical non-negative tensor factorization (HNTF) is obtained by adopting the local objective function and the theory of three semi-NMF. Its application in mechanical fault feature extraction and diagnosis is explored.

1 HNTF Algorithm

1.1 Three semi-NMF theory

Taking a three-order tensor into consideration, we can describe the NTF model as follows[5]. For a given non-negative tensor $\boldsymbol{G} \in \mathbf{R}_{+}^{d_1 \times d_2 \times d_3}$, the objective is to find matrices $\boldsymbol{U} \in \mathbf{R}_{+}^{d_1 \times k}$, $\boldsymbol{V} \in \mathbf{R}_{+}^{d_2 \times k}$, $\boldsymbol{W} \in \mathbf{R}_{+}^{d_3 \times k}$ by solving Eq. (1) with the purpose of minimizing the reconstruction error $\boldsymbol{E}$ and ensuring non-negative restriction of $\boldsymbol{U}$, $\boldsymbol{V}$, $\boldsymbol{W}$.

$$\boldsymbol{G} = \sum_{j=1}^{k} \boldsymbol{u}^j \circ \boldsymbol{v}^j \circ \boldsymbol{w}^j + \boldsymbol{E} \tag{1}$$

$$D_{\mathrm{F}}(\boldsymbol{G} \parallel [\boldsymbol{U}, \boldsymbol{V}, \boldsymbol{W}]) = \frac{1}{2} \left\| \boldsymbol{G} - \sum_{j=1}^{k} \boldsymbol{u}^j \circ \boldsymbol{v}^j \circ \boldsymbol{w}^j \right\|_{\mathrm{F}}^2 \tag{2}$$

$$\text{s.t. } \boldsymbol{u}^j, \boldsymbol{v}^j, \boldsymbol{w}^j \geqslant 0$$

where $\boldsymbol{u}^j$, $\boldsymbol{v}^j$, and $\boldsymbol{w}^j$ are the j-th column of $\boldsymbol{U}$, $\boldsymbol{V}$, $\boldsymbol{W}$, respectively. Thus, the NTF can be deformed into a Euclidean distance-based least squares problem with non-negative constraints.

Zhang et al.[6] first proposed the three semi-NMF theory. Introducing Khatri-Rao Θ and Kronecker $\otimes$, for Eq. (2), the Khatri-Rao product of two matrices is defined as $\boldsymbol{U}\Theta\boldsymbol{V} = [\boldsymbol{u}^1 \otimes \boldsymbol{v}^1 \quad \cdots \quad \boldsymbol{u}^k \otimes \boldsymbol{v}^k] \in \mathbf{R}_{+}^{d_1 d_2 \times k}$. Similarly, the Khatri-Rao product of two vectors is $\boldsymbol{u}^j \Theta \boldsymbol{v}^j = \boldsymbol{u}^j \otimes \boldsymbol{v}^j = \{(\boldsymbol{u}_1^j \boldsymbol{v}^j)^{\mathrm{T}}, (\boldsymbol{u}_2^j \boldsymbol{v}^j)^{\mathrm{T}}, \ldots, (\boldsymbol{u}_{d_1}^j \boldsymbol{v}^j)^{\mathrm{T}}\}^{\mathrm{T}} \in \mathbf{R}_{+}^{d_1 d_2}$. Here, $\boldsymbol{u}_i^j$ is the component of

Received 2011-07-31.

Biographies: Wang Fei (1985—), male, graduate; Xu Feiyun (corresponding author), male, doctor, professor, fyxu@seu.edu.cn.

Foundation items: The National Natural Science Foundation of China (No. 50875078), the Natural Science Foundation of Jiangsu Province (No. BK2007115), the National High Technology Research and Development Program of China (863 Program) (No. 2007AA04Z421).

Citation: Wang Fei, Xu Feiyun, Wang Haijun. Local hierarchical non-negative tensor factorization and its application in machinery fault diagnosis [J]. Journal of Southeast University (English Edition), 2011, 27(4): 394 – 399. [doi: 10.3969/j.issn.1003 – 7985.2011.04.010]

the vector $\boldsymbol{u}^j$. Then Eq. (2) can be transformed into three sub-equivalent objective function formulae:

$$\left.\begin{aligned} D_U(\boldsymbol{G}_1 \parallel \boldsymbol{U}(\boldsymbol{W}\Theta\boldsymbol{V})^{\mathrm{T}}) &= \frac{1}{2}\parallel \boldsymbol{G}_1 - \boldsymbol{U}(\boldsymbol{W}\Theta\boldsymbol{V})^{\mathrm{T}} \parallel_{\mathrm{F}}^2 \\ D_V(\boldsymbol{G}_2 \parallel \boldsymbol{V}(\boldsymbol{W}\Theta\boldsymbol{U})^{T}) &= \frac{1}{2}\parallel \boldsymbol{G}_2 - \boldsymbol{V}(\boldsymbol{W}\Theta\boldsymbol{U})^{\mathrm{T}} \parallel_{\mathrm{F}}^2 \\ D_W(\boldsymbol{G}_3 \parallel \boldsymbol{W}(\boldsymbol{V}\Theta\boldsymbol{U})^{T}) &= \frac{1}{2}\parallel \boldsymbol{G}_3 - \boldsymbol{W}(\boldsymbol{V}\Theta\boldsymbol{U})^{\mathrm{T}} \parallel_{\mathrm{F}}^2 \end{aligned}\right\} \quad (3)$$

where $\boldsymbol{G}_1 \in \mathbf{R}_+^{d_2d_3\times d_1}$, $\boldsymbol{G}_2 \in \mathbf{R}_+^{d_1d_3\times d_2}$, $\boldsymbol{G}_3 \in \mathbf{R}_+^{d_1d_2\times d_3}$ are two-dimensional transformed matrices of $\boldsymbol{G}$. Fixing $\boldsymbol{W}\Theta\boldsymbol{V}$, $\boldsymbol{W}\Theta\boldsymbol{U}$, $\boldsymbol{V}\Theta\boldsymbol{U}$ and seeking $\boldsymbol{U}$, $\boldsymbol{V}$, $\boldsymbol{W}$ separately, the normal NTF algorithm is obtained based on the three semi-NMF theory, by which Ji[7] first proved the identity of NMF and NTF.

1.2 Local objective function

Cichock et al.[8] referred to the concept of local objective function, and applied it to the least-squares NMF algorithms. The core idea is to define the local matrix. For a given non-negative matrix $\boldsymbol{V}$ and its factorized matrices of $\boldsymbol{W}, \boldsymbol{H}$, the local matrix is defined as

$$\begin{aligned} \boldsymbol{V}^{(j)} &= \boldsymbol{V} - \sum_{l\neq j}\boldsymbol{w}_l\boldsymbol{h}_l = \boldsymbol{V} - \boldsymbol{W}\boldsymbol{H} + \boldsymbol{w}_j\boldsymbol{h}_j = \\ &\quad \boldsymbol{E} + \boldsymbol{w}_j\boldsymbol{h}_j \qquad j = 1,2,\cdots,J \end{aligned} \quad (4)$$

Thus, local objective functions are

$$D_{\boldsymbol{w}}^{(j)}(\boldsymbol{w}_j) = \frac{1}{2}\parallel \boldsymbol{V}^{(j)} - \boldsymbol{w}_j\boldsymbol{h}_j \parallel_{\mathrm{F}}^2 \qquad \text{for } \boldsymbol{w}_j, \text{ fixed } \boldsymbol{h}_j \quad (5)$$

$$D_{\boldsymbol{h}}^{(j)}(\boldsymbol{h}_j) = \frac{1}{2}\parallel \boldsymbol{V}^{(j)} - \boldsymbol{w}_j\boldsymbol{h}_j \parallel_{\mathrm{F}}^2 \qquad \text{for } \boldsymbol{h}_j, \text{ fixed } \boldsymbol{w}_j \quad (6)$$

The matrix decomposition results can be obtained by solving Eqs. (5) and (6).

1.3 HNTF

Owing to the use of the least squares and not the gradient descent method for solving the problem in Ref. [8], which leads to the discontinuous convergence, we cannot achieve a high decomposition accuracy. Introducing the idea of local objective function, we use the gradient descent method to solve the NTF problem.

For the NTF model, by applying the local function theory to Eq. (3), the local tensor can be defined as

$$\boldsymbol{G}^j = \boldsymbol{G} - \sum_{\substack{l=1\\ l\neq j}}^{k}\boldsymbol{u}^l\circ\boldsymbol{v}^l\circ\boldsymbol{w}^l \quad (7)$$

The local objective functions of Eq. (3) are

$$\left.\begin{aligned} D_{\boldsymbol{u}^j}(\boldsymbol{G}_1^j \parallel \boldsymbol{u}^j(\boldsymbol{w}^j\Theta\boldsymbol{v}^j)^{\mathrm{T}}) &= \frac{1}{2}\parallel \boldsymbol{G}_1^j - \boldsymbol{u}^j(\boldsymbol{w}^j\Theta\boldsymbol{v}^j)^{\mathrm{T}} \parallel_{\mathrm{F}}^2 \\ D_{\boldsymbol{v}^j}(\boldsymbol{G}_2^j \parallel \boldsymbol{v}^j(\boldsymbol{w}^j\Theta\boldsymbol{u}^j)^{\mathrm{T}}) &= \frac{1}{2}\parallel \boldsymbol{G}_2^j - \boldsymbol{v}^j(\boldsymbol{w}^j\Theta\boldsymbol{u}^j)^{\mathrm{T}} \parallel_{\mathrm{F}}^2 \\ D_{\boldsymbol{w}^j}(\boldsymbol{G}_3^j \parallel \boldsymbol{w}^j(\boldsymbol{v}^j\Theta\boldsymbol{u}^j)^{\mathrm{T}}) &= \frac{1}{2}\parallel \boldsymbol{G}_3^j - \boldsymbol{w}^j(\boldsymbol{v}^j\Theta\boldsymbol{u}^j)^{\mathrm{T}} \parallel_{\mathrm{F}}^2 \end{aligned}\right\} \quad (8)$$

First, fixing $\boldsymbol{w}^j\Theta\boldsymbol{v}^j$, $\boldsymbol{v}^j\Theta\boldsymbol{u}^j$, and $\boldsymbol{w}^j\Theta\boldsymbol{u}^j$, we derive $\boldsymbol{u}^j$, $\boldsymbol{v}^j$, and $\boldsymbol{w}^j$ by Eq. (8). Secondly, we adopt the gradient descent method and select the negative gradient direction and then let

$$\left.\begin{aligned} \boldsymbol{u}^j &= \boldsymbol{u}^j - \mu_{\boldsymbol{u}^j}\nabla_{\boldsymbol{u}^j} = \\ &\quad \boldsymbol{u}^j - \mu_{\boldsymbol{u}^j}(\boldsymbol{u}^j(\boldsymbol{w}^j\Theta\boldsymbol{v}^j)^{\mathrm{T}}(\boldsymbol{w}^j\Theta\boldsymbol{v}^j) - \boldsymbol{G}_1^{(j)}(\boldsymbol{w}^j\Theta\boldsymbol{v}^j)) \\ \boldsymbol{v}^j &= \boldsymbol{v}^j - \mu_{\boldsymbol{v}^j}\nabla_{\boldsymbol{v}^j} = \\ &\quad \boldsymbol{v}^j - \mu_{\boldsymbol{v}^j}(\boldsymbol{v}^j(\boldsymbol{w}^j\Theta\boldsymbol{u}^j)^{\mathrm{T}}(\boldsymbol{w}^j\Theta\boldsymbol{u}^j) - \boldsymbol{G}_2^{(j)}(\boldsymbol{w}^j\Theta\boldsymbol{u}^j)) \\ \boldsymbol{w}^j &= \boldsymbol{w}^j - \mu_{\boldsymbol{w}^j}\nabla_{\boldsymbol{w}^j} = \\ &\quad \boldsymbol{w}^j - \mu_{\boldsymbol{w}^j}(\boldsymbol{w}^j(\boldsymbol{v}^j\Theta\boldsymbol{u}^j)^{\mathrm{T}}(\boldsymbol{v}^j\Theta\boldsymbol{u}^j) - \boldsymbol{G}_3^{(j)}(\boldsymbol{v}^j\Theta\boldsymbol{u}^j)) \end{aligned}\right\} \quad (9)$$

Suppose that

$$\left.\begin{aligned} \mu_{\boldsymbol{u}^j} &= \frac{\boldsymbol{u}^j}{\boldsymbol{u}^j(\boldsymbol{w}^j\Theta\boldsymbol{v}^j)^{\mathrm{T}}(\boldsymbol{w}^j\Theta\boldsymbol{v}^j)} \\ \mu_{\boldsymbol{v}^j} &= \frac{\boldsymbol{v}^j}{\boldsymbol{v}^j(\boldsymbol{w}^j\Theta\boldsymbol{u}^j)^{\mathrm{T}}(\boldsymbol{w}^j\Theta\boldsymbol{u}^j)} \\ \mu_{\boldsymbol{w}^j} &= \frac{\boldsymbol{w}^j}{\boldsymbol{w}^j(\boldsymbol{v}^j\Theta\boldsymbol{u}^j)^{\mathrm{T}}(\boldsymbol{v}^j\Theta\boldsymbol{u}^j)} \end{aligned}\right\} \quad (10)$$

Finally, the iterative formulae are obtained as

$$\left.\begin{aligned} \boldsymbol{u}^j &= \boldsymbol{u}^j \cdot^* (\boldsymbol{G}_1^j(\boldsymbol{w}^j\Theta\boldsymbol{v}^j)) \cdot/ (\boldsymbol{u}^j(\boldsymbol{w}^j\Theta\boldsymbol{v}^j)^{\mathrm{T}}(\boldsymbol{w}^j\Theta\boldsymbol{v}^j)) \\ \boldsymbol{v}^j &= \boldsymbol{v}^j \cdot^* (\boldsymbol{G}_2^j(\boldsymbol{w}^j\Theta\boldsymbol{u}^j)) \cdot/ (\boldsymbol{v}^j(\boldsymbol{w}^j\Theta\boldsymbol{u}^j)^{\mathrm{T}}(\boldsymbol{w}^j\Theta\boldsymbol{u}^j)) \\ \boldsymbol{w}^j &= \boldsymbol{w}^j \cdot^* (\boldsymbol{G}_3^j(\boldsymbol{v}^j\Theta\boldsymbol{u}^j)) \cdot/ (\boldsymbol{w}^j(\boldsymbol{v}^j\Theta\boldsymbol{u}^j)^{\mathrm{T}}(\boldsymbol{v}^j\Theta\boldsymbol{u}^j)) \end{aligned}\right\} \quad (11)$$

where $\cdot^*$ and $\cdot/$ are the corresponding elements multiplication and division of vectors or matrices. Due to the possibility that negative elements exist in $\boldsymbol{G}^j$, it is required to impose the non-negative constraints of $\boldsymbol{u}^j, \boldsymbol{v}^j, \boldsymbol{w}^j$ in the iterative process.

The process of the HNTF algorithm is as follows:

1) Initialize $\boldsymbol{U}, \boldsymbol{V}, \boldsymbol{W}$ by random non-negative values and normalize $\boldsymbol{U}, \boldsymbol{V}$.

2) Compute reconstruction error tensor $\boldsymbol{E} = \boldsymbol{G} - \sum_{j=1}^{k}\boldsymbol{u}^j\circ\boldsymbol{v}^j\circ\boldsymbol{w}^j$.

3) For $j = 1,2,\cdots,J$, compute $\boldsymbol{G}^j = \boldsymbol{E} + \boldsymbol{u}^j\circ\boldsymbol{v}^j\circ\boldsymbol{w}^j$ in turn and solve Eq. (11). Impose non-negative constraints and then normalize $\boldsymbol{u}^j, \boldsymbol{v}^j$.

4) Repeat step 2) and step 3) until a stopping criterion is met.

2 Algorithm Verification

The MIT face database created by the MIT Media Lab is used here, consisting of 2 429 gray images of 16 volunteers with different poses, illuminations and sizes. In this way, a tensor with a size of $19\times19\times2\,429$ is obtained, and then it is decomposed by the methods of NTF and HNTF. The number of the extracted facial features is assumed to be 25. The results are shown in Figs. 1 and 2.

As shown in Figs. 1 (a) and (b), local features of the face images extracted by the HNTF are more sparse and clear at the same iterations. As can be seen from Fig. 2, after the 7th step, the HNTF achieves the same precision as that attained by the NTF after the 100th step and it improves the convergence significantly.

3 Fault Feature Extraction of Air Compressor Based on HNTF

3.1 Analysis of air compressor's spectral and bispectral properties

The vibration signal data of a high-speed shaft of a

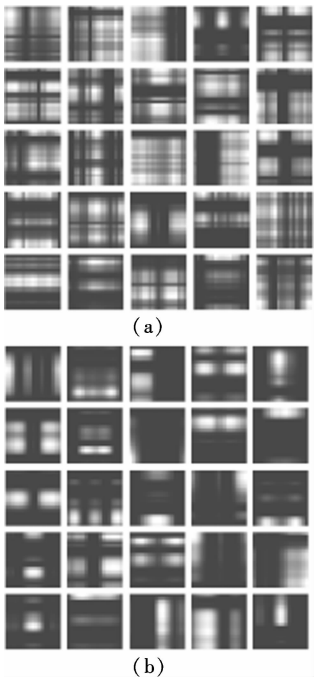

Fig. 1 Basis images of the face extracted by different methods. (a) NTF; (b) HNTF

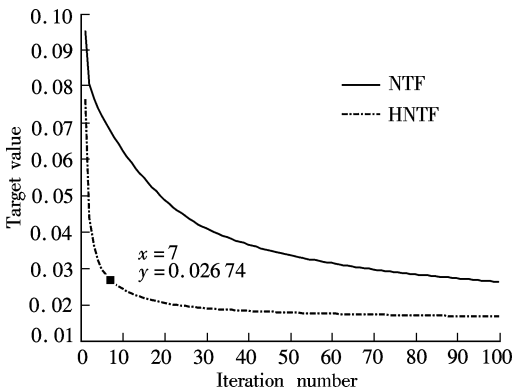

Fig. 2 Relationship between iteration number and target value

centrifugal compressor is used. The fundamental (first harmonic) frequency is 385.742 2 Hz and the sampling frequency is 4 900 Hz. The vibration data including 180 groups of signals are collected when the compressor is under the conditions of three typical faults (rotor imbalance, oil whirl and loose fastener). The spectral properties of different faults are shown as follows.

When the rotor imbalance fault occurs, the fundamental amplitude increases significantly. During the oil whirl, both the amplitudes of the 1/2 of the fundamental and the fundamental increase[9]. When the loose fasteners occur, not only do the amplitudes of the 0.35-0.45 and $1/n$ (n changes with the location and severity of the fault) of the fundamental increase with the increase of the fundamental amplitude, but also the second harmonic amplitude increases significantly. Furthermore, higher harmonic components also exist when the fault of loose fasteners occurs. The various fault spectrums are shown in Fig. 3.

The spectrum analysis method is simple, but it cannot extract the nonlinear characteristics, it loses the phase information of the signal, and it is sensitive to noise interference.

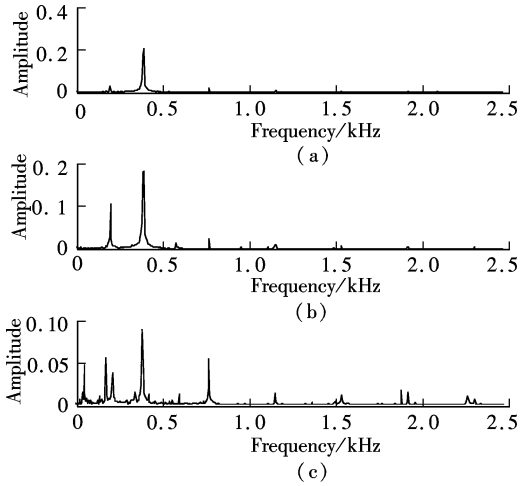

Fig. 3 Different fault spectrums. (a) Imbalance; (b) Oil whirl; (c) Loose fastener

In contrast, higher-order spectra of signals are non-sensitive to additive Gaussian and symmetric non-Gaussian noise. Meanwhile, it can detect the phase coupling information of signals[10]. So it has been more and more applied to the fault feature extraction of mechanical systems. Taking the bispectrum for example, the bispectrum images of three typical faults are shown in Fig. 4.

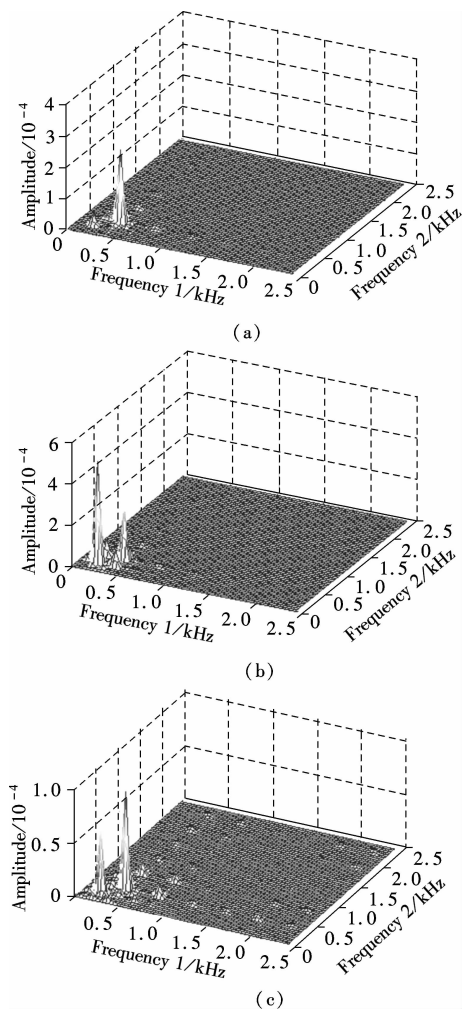

Fig. 4 Bispectrum of three typical faults. (a) Imbalance; (b) Oil whirl; (c) Loose fasteners

3.2 Feature extraction and fault diagnosis based on bispectrum

The process of feature extraction and fault diagnosis based on bispectrum is as follows:

1) Deform the m signals $x(t)$ in bispectrum and then form the non-negative tensor $\boldsymbol{G}$.

2) Set the basis dimension and factorize $\boldsymbol{G}$. Compute the basis images $\boldsymbol{u}^j\boldsymbol{v}^{j\mathrm{T}}$, $j = 1, 2, \cdots, k$ and the corresponding weight matrix $\boldsymbol{W}$.

3) Divide $\boldsymbol{W}$ into training samples $\boldsymbol{W}_{\text{train}}$ and testing samples $\boldsymbol{W}_{\text{test}}$. Input $\boldsymbol{W}_{\text{train}}$ into the BP neural network and then import $\boldsymbol{W}_{\text{test}}$ into the trained BP neural network. Finally, inspect the fault classification rate.

Frequency pairs shown in Fig. 5 are (385,385), (153, 230), (230,153), (192,192), (427,343), (343,427) (in Hz). In addition, (385,770) and (770,385) are also included in the basis images of Figs. 5(a) and (e). Expect for the frequency pairs mentioned above, the frequency pairs of (42,42), (153,42), (42,153) and others can also be seen in the basis images of Figs. 5(b), (c) and (f). The rotor imbalance fault is reflected by the frequency pair of (385,385), while the oil whirl is mainly expressed by the (192,192). The frequency of 343 and 427 represent the difference frequency and the sum frequency of the fundamental frequency and 1/9 of the fundamental, respectively. In the same manner, the frequency of 153 (also the 0.35-0.45 of the fundamental approximately) and 230 are the difference frequency and the sum frequency of the 1/2 and 1/9 of the fundamental, respectively. All of them reflect the second phase coupling relationships between various frequencies when the oil whirl occurs. There are also frequency pairs (42, 42) (1/9 of the fundamental), (385,770) and (770, 385). They reflect the characteristics of the fastener looseness fault altogether. In contrast, we mainly obtain the frequency pairs of (192, 192), (385, 385), (230,153), (347, 427) in Fig. 6. Therefore, the second phase coupling information is not expressed clearly compared with Fig. 5. Nevertheless, in Fig. 7, we can only find the traditional frequency pairs such as the (385, 385), (770,385), (385,770), (192,192), (42,42) and some other useless frequencies caused by incorrect composition.

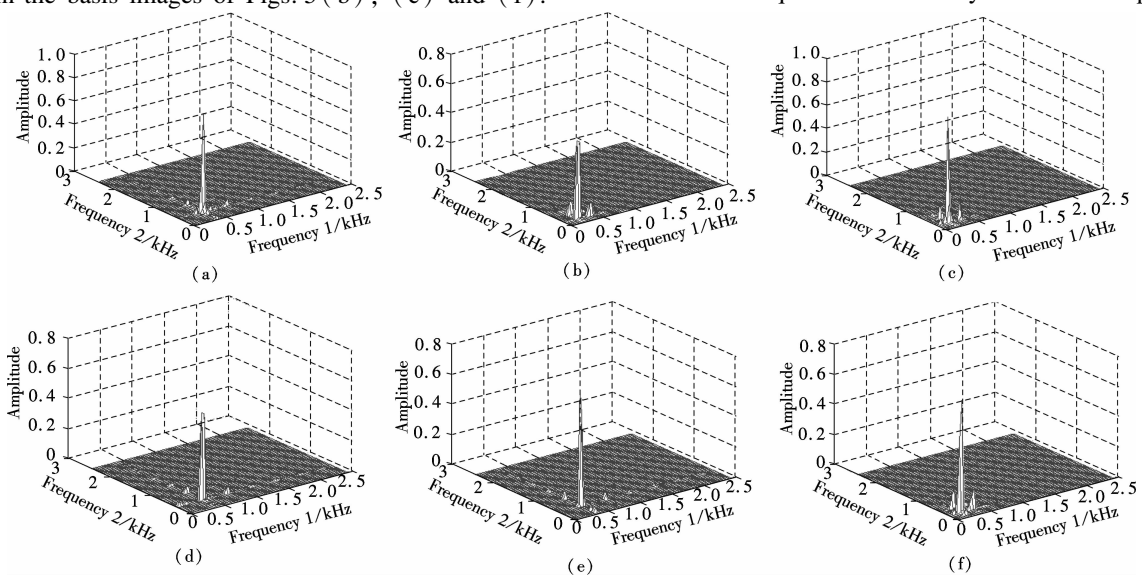

Fig. 5 Basis images extracted by HNTF

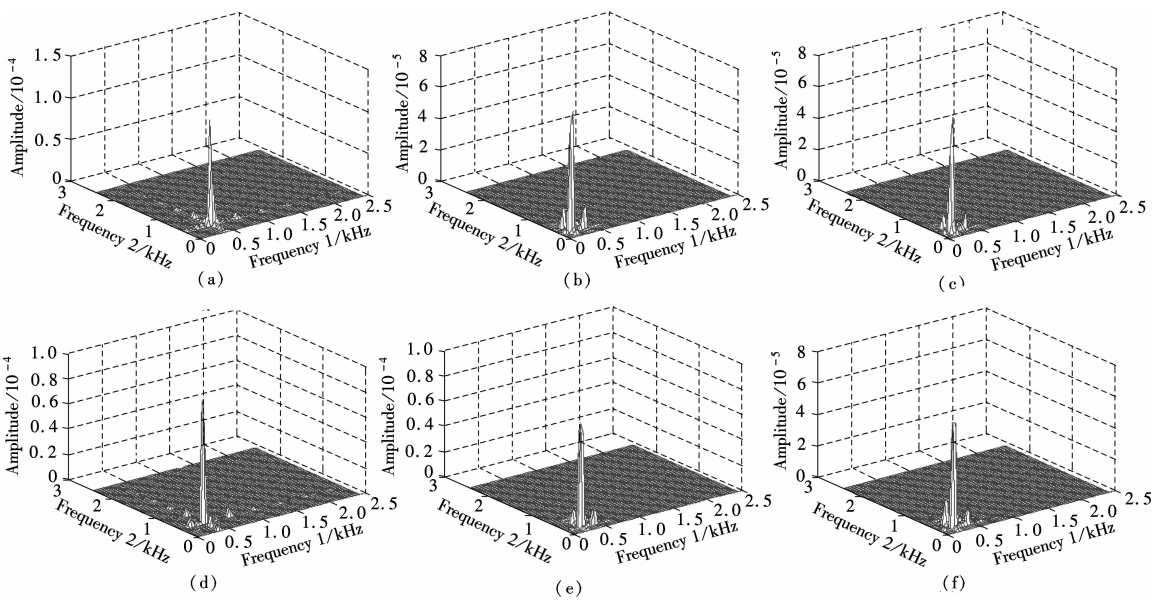

Fig. 6 Basis images extracted by NTF

The frequency pairs (230,153), (153,230), (347,427), (427,347) reflecting the second phase coupling information cannot be seen at all. Furthermore, the accuracy of decomposition is not high as shown in Tab. 1.

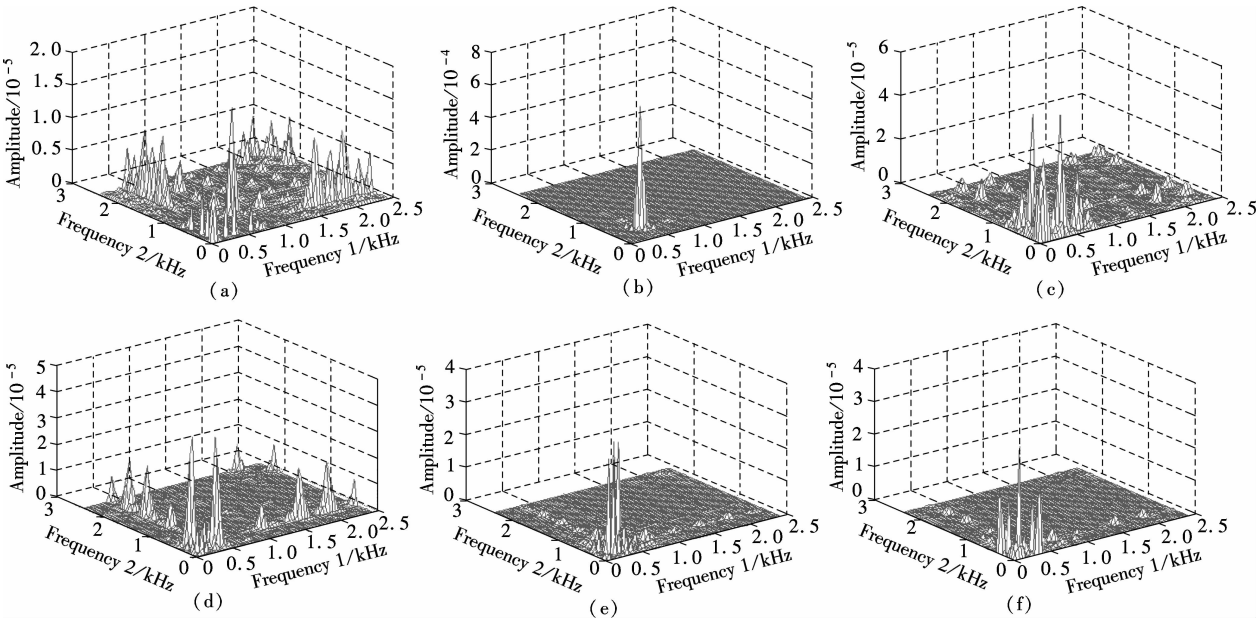

Fig. 7 Basis images extracted by PCA

Tab. 1 Comparison of different factorization algorithms

Algorithm	Basis dimension	Computation time	Target value
NTF	6	210.328	0.012 5
HNTF	6	101.594	0.006 0
PCA	6		0.735 3

As listed in Tab. 1, the decomposition rate of the HNTF is improved. At the same time, by applying the local objective function to strike a negative direction, the decomposition accuracy is increased.

Since the weights of the characteristics are stored in the weight matrix $\boldsymbol{W}$, we build the BP neural network through the divided samples and import the test samples $\boldsymbol{W}_{\text{test}}$ into the trained neural networks through $\boldsymbol{W}_{\text{train}}$ so as to distinguish the types of different faults. The diagnosis results are listed in Tab. 2. It can be seen that the fault recognition rates by the HNTF are the highest compared with the NTF and PCA methods.

Tab. 2 Fault diagnosis recognition rates of different methods

Algorithm	Average recognition rate			Total average recognition rate
	Imbalance	Oil whirl	Loose fasteners	
NTF	0.694	0.767	1.000	0.821
HNTF	0.964	0.776	1.000	0.913
PCA	0.611	0.629	0.831	0.690

4 Conclusion

The hierarchical non-negative tensor factorization method based on the local objective function is proposed, which can reduce the number of iterative steps and improve the convergence and the precision of the NTF. Its validity is verified by face data experiments. The proposed method is applied to the fault features extraction and fault diagnosis of an air compressor. Results show that the algorithm can efficiently improve the accuracy of fault diagnosis compared with the traditional feature extraction methods.

References

[1] Hazan T, Polak S, Shashua A. Sparse image coding using a 3D non-negative tensor factorization [C]//*Proceedings of the Tenth IEEE International Conference on Computer Vision*. Beijing, China, 2005:50 - 57.

[2] Cichocki A, Phan A H, Caiafa C. Flexible HALS algorithms for sparse non-negative matrix/tensor factorization [C]//*Proceedings of* 2008 *IEEE International Workshop on Machine Learning for Signal Processing*. Cancun, Mexico, 2008: 73 - 78.

[3] Heiler M, Schnörr C. Controlling sparseness in non-negative tensor factorization [C]//*The Ninth European Conference on Computer Vision*. Graz, Austria, 2006: 56 - 67.

[4] Park S W, Savvides M. Estimating mixing factors simultaneously in multilinear tensor decomposition for robust face recognition and synthesis [C]//*Proceedings of the* 2006 *IEEE Conference on Computer Vision and Pattern Recognition Workshop*. New York, USA, 2006: 49 - 55.

[5] Peng Sen. Research on mechanical fault feature extraction based on non-negative tensor factorization [D]. Nanjing: School of Mechanical Engineering of Southeast University, 2010. (in Chinese)

[6] Zhang Q, Wang H, Plemmons R J, et al. Tensor methods for hyperspectral data analysis: a space object material identification study[J]. *Journal of the Optical Society of America A: Optics, Image Science, and Vision*, 2008, **25**(12): 3001 - 3012.

[7] Ji Jinlu. Research on mechanical fault feature extraction theories and methods based on non-negative factorization[D]. Nanjing: School of Mechanical Engineering of Southeast University, 2011. (in Chinese)

[8] Cichocki A, Zdunek R, Amari S I. Hierarchical ALS algorithms for nonnegative matrix and 3D tensor factorization [C]//*Proceedings of the Seventh International Conference on Independent Component Analysis and Signal Separation*. London, UK, 2007:169 - 176.

[9] Zhang Jianzhong. The common typical faults' mechanism and characteristics analysis of the rotating machinery[J]. *Guangxi Light Industry*, 2008(7): 32 - 33. (in Chinese)

[10] Ma Jiancang, Niu Yilong, Chen Haiyang. *Blind signal processing*[M]. Beijing: National Defence Industry Press, 2006:38 - 44. (in Chinese)

局部分层非负张量分解算法及在机械故障诊断中的应用

王 飞[1] 许飞云[2] 王海军[2]

(东南大学机械工程学院,南京 211189)

摘要:针对传统非负张量分解收敛速度慢,分解精度低的难题,结合 three semi-NMF 模型,将局部目标函数理论应用于非负张量分解中,提出了基于局部分层的非负张量分解算法,并通过人脸特征提取实验验证了算法的有效性. 通过对由空压机不同故障振动信号的双谱构成的张量按该算法分解,得到反映故障特征的基图像及与基图像对应的权值矩阵,建立了特征与故障频率之间的对应关系,并将权值矩阵输入到 BP 神经网络中对故障进行分类. 同时将该方法与其他特征提取方法相比较,实验结果表明该方法有效地提高了空压机故障诊断精度.

关键词:非负张量分解;双谱;特征提取;空压机;BP 神经网络

中图分类号:TP206. 3